ISSN: 0975 -8542

Journal of Global Pharma Technology

Available Online at: www.jgpt.co.in

RESEARCH ARTICLE

# Investigation Structural Properties of $Cu_2ZnSnS_4$Thin Films Prepared by Pulse Laser Deposition

**Ali J. Khalaf*, Nahida B. Hassan**

*Physics Depart. /College of Science/Babylon University/Iraq.*

***Correspondence Author: Ali J. Khalaf**

## Abstract

The prepared samples of thin-film by laser ablation method were achieved. Powders of (CZTS) copper (Cu), zinc (Zn), tin (Sn) and Sulfur (S) of and then compressing by approximately 3 tons in Pellets form. The samples were ablated by using Neodymium-YAG laser with different laser energies (400mJ, 500mJ, 600mJ, 700mJ, 800mJ) and number of pulses (300) pulse, frequency (6Hz) and wavelength (1064) nm obtained the plasma plume at $10^{-5}$mbar pressure. Results indicate by using XRD, AFM , SEM and EDX devices.by x-ray diffraction study of $Cu_2ZnSnS_4$ compound films prepared are proven to be polycrystalline tetragonal as noted when the laser energy is increased when the process of ablation of the target CZTS The grain size increases while the strain, the dislocation density and the lattice constants ($a_o$, $c_o$) decrease. Through the images of the atomic force microscope (AFM) it was observed that the grain size decreases from ($CZTS_{400mJ}$-$CZTS_{700mJ}$) and then increases. There is also an increase in the surface roughness rate and the square root rate ($CZTS_{600mJ}$ - $CZTS_{800mJ}$) by increasing the laser energy when the process of ablation of the target CZTS with constant other laser parameters. Through scanning electron microscopy (SEM) images, the spherical shape of the nanoparticles is observed by increasing the laser energy when the process of ablation of the target CZTS with constant other laser parameters with irregular forms. The EDX test showed that the films contained Cu, Zn, Sn, S elements as expected, indicating the formation of high-purity CZTS films.

**Keywords:** *Structural, Thin film, Nanoparticle, CZTS, Composite, XRD, AFM, SEM, EDX, laser ablation.*

## Introduction

Is a quaternary semiconducting compound Includes I2-II-IV-VI4 aggregates such as copper (Cu), zinc (Zn), tin (Sn) and Sulfur (S), The CZTS can be obtained by replacing the trivalent In / Ga element with divalent Zn and tetravalent Sn which form the kesterite phase [1]. CZTS is a glycoprotein compound used as a sorbent in solar cells [2].

It was discovered more than twenty years ago by researchers Ito Nakazawa [3] they were able to prepare this compound as a thin film using spray technology. This compound has a direct energy gap of about 1.4 - 1.5eV and has an absorption coefficient in the visible area greater than ($10^4 cm^{-1}$) and a positive conductivity [4], it's very low cost compared to light absorbing compounds such as Cu (InGa) (S, Se), CuInS2 [5]. High thermal stability as well as the use does not affect the environment due to the lack of noble elements and very toxic substances, The composition of Cu2ZnSnS4 consists of a quadrilateral type This compound has been prepared in several different ways [6].

### Practical Part

To prepare the thin films of $Cu_2ZnSnS_4$ of different laser energies (400mJ, 500mJ, 600mJ, 700mJ, 800mJ) by using laser ablation system which consists of two parts, the first part of discharge chamber that contains the target holder and holder for substrate and a window for the passage of the laser light made light of the pack quartz, as well as thermal and double valves dump, where it is the subject of substrate vertically on the target holder, where the distance between them is 4cm and the pressure inside the room deposition $10^{-5}$ mill bars, which can be accessed using the discharge rotary and diffusion vacuum respectively.

©2009-2020, JGPT. All Rights Reserved

The second part consists of a system of Nd-YAG laser which operates at wavelength 1064nm, and using energies (400mJ, 500mJ, 600mJ, 700mJ, 800mJ) for five samples and 6 HZ frequency and number of pulses used was 300 pulses constant. The laser beam is focused on the target using the focal lens dimension to distant subjects 30cm inclination angle almost $45^0$ surface.

The powders of pure CZTS materials are, then compressed these powders using hydraulic piston, under pressure 3Ton, getting tablets thickness 3 mm, diameter of 2 cm. It was placed inside the deposition chamber on the target holder, ablated these discs using a laser Nd-YAG focused of the laser beam on the target using the lens focal dimension 30cm surface. The thin films prepared were examined by XRD, AFM SEM and an EDX.

## Results and Discussion

The synthesis of the prepared films (CZTS) was identified by 300 pulse laser pulses, 1064 nm wavelength and different laser energies (400mJ, 500mJ, 600mJ, 700mJ, 800mJ). It was found to have a polycrystalline and Tetragonal polycrystalline structure at crystalline levels (112) (206) (112) at angles ($2\Theta = 41.96^{o}$), ($2\Theta = 40.4^{o}$) and ($2\Theta = 28.4^{o}$) respectively.

When the laser energy is increased, and the other laser parameters are constant represented by The number of pulses and the wavelength We noticed a rise in the peaks and became sharp for the crystal levels and the appearance of the peak at the angle ($2\Theta = 28.49^{o}$) which returns to the crystal level (112) the results obtained from X-ray diffraction were confirmed with ICDD (International Center for Diffraction Data) card number (96-900-4751). We observed that the prevailing trend is (112) when laser energies change from 400 mJ to 500 mJ and other preparation conditions are constant. When increasing the laser energies, we observed an increase in the peaks relative to the crystalline levels with a decrease in the value of FWHM this indicates an increase in grain size.

The effect of laser energy on the grain size rate calculated using the FWHM Scherrer equation was also studied. This is due to the increased energies of the laser, the crystallization increases and therefore the grain boundaries are reduced as a result of the occupation of the largest number of atoms of the deposition, causing a decrease in the value of FWHM because when you increase the energies of the laser increases the kinetic energy of atoms (CZTS) This facilitates the occupation of atoms located in the crystalline lattice.

The increase in laser energies results in a small decrease in the value of the lattice constants this is due to a decrease in the value of the distance between crystalline levels ($d_{hkl}$) with the increase of laser energies We noted that the stress decreases when the laser energies increase, causing an increase in grain size. As we also noted, the dislocations density decreases with increasing laser energies, as in Table (1-1) and decreases with increasing grain size. Because the relationship between them is inverse and that means an improvement in the crystal structure, i.e. in the grain size as shown in Figures (1.1), (1.2), (1.3), (1.4) and (1.5).

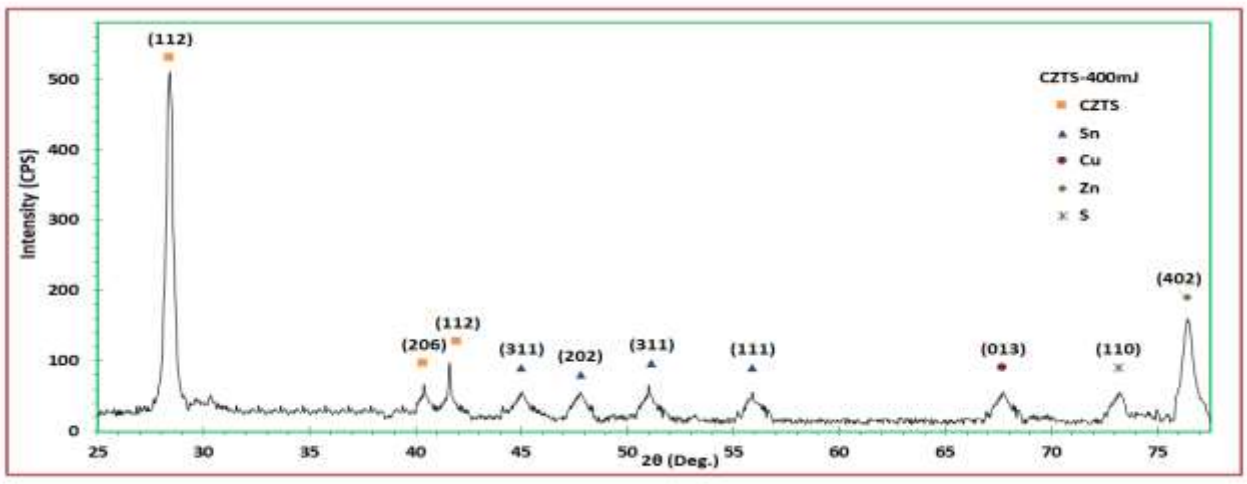


**Figure 1.1: X-ray diffraction of CZTS films prepared with 300 pulses, 1064 nm wavelength and 400 mJ laser energy**

©2009-2020, JGPT. All Rights Reserved 

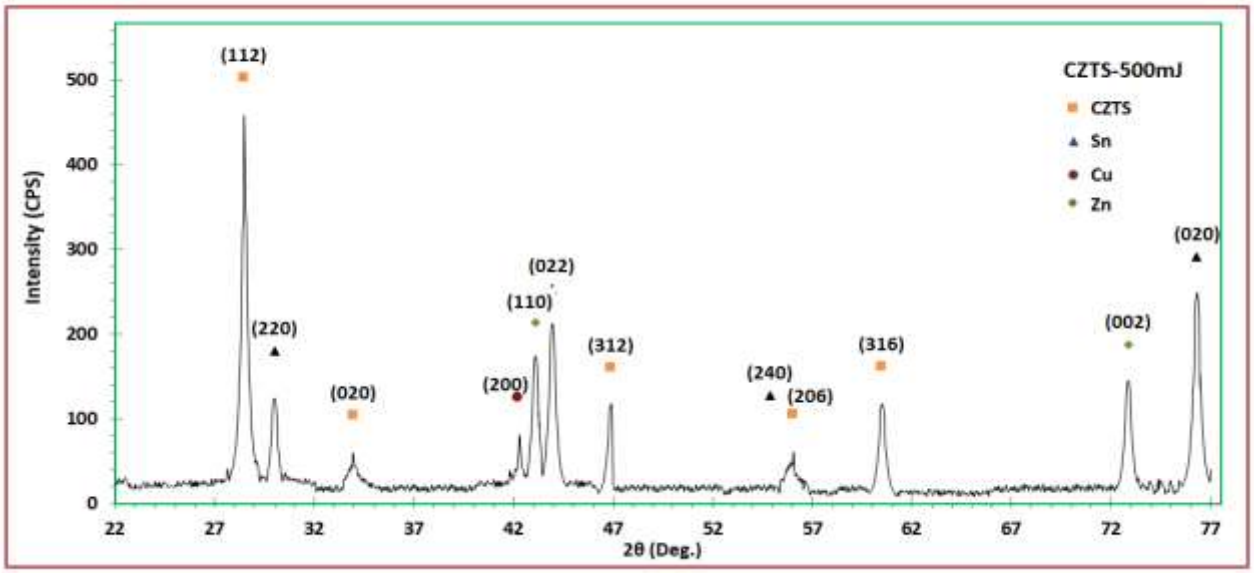


**Figure 1.2: X-ray diffraction of CZTS films prepared with 300 pulses, 1064 nm wavelength and 500 mJ laser energy**

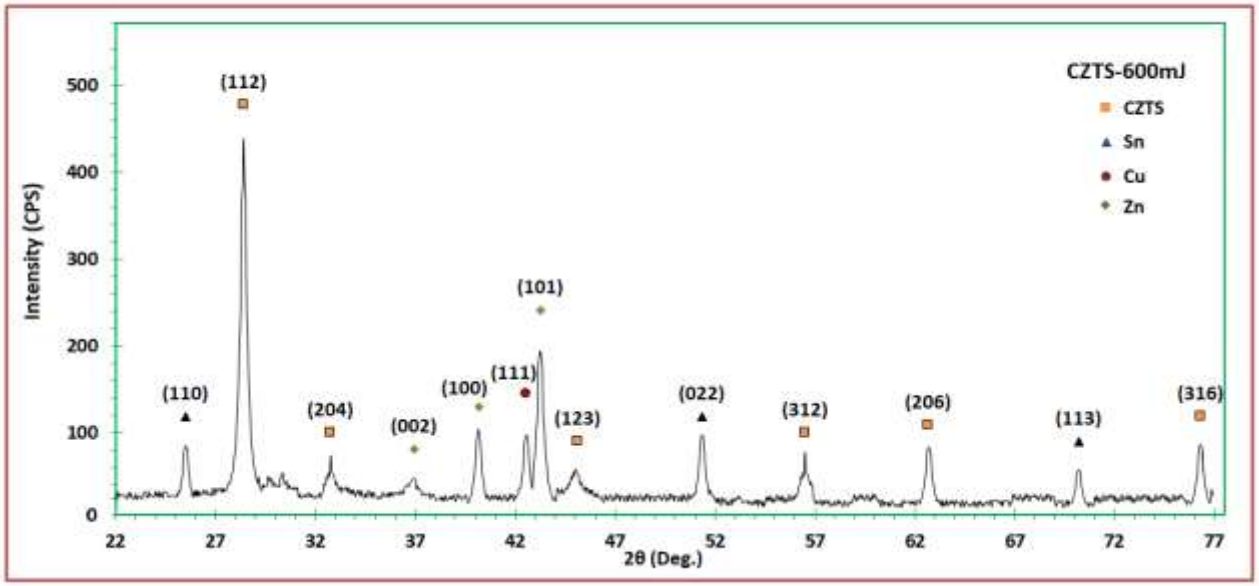


**Figure 1.3: X-ray diffraction of CZTS films prepared with 300 pulses, 1064 nm wavelength and 600 mJ laser energy**

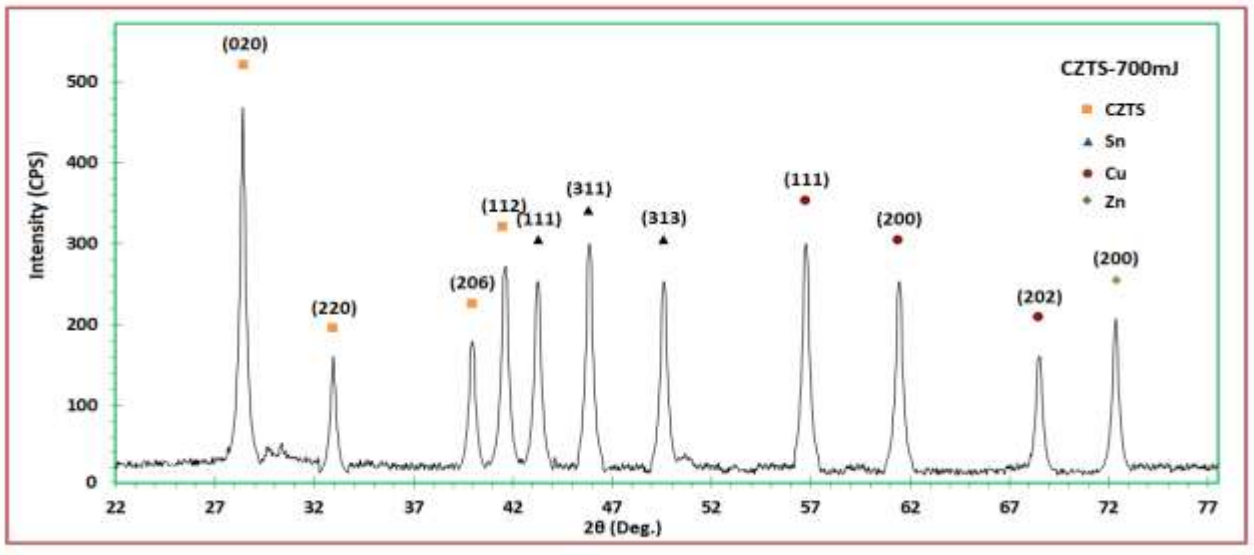


**Figure 1.4: X-ray diffraction of CZTS films prepared with 300 pulses, 1064 nm wavelength and 700 mJ laser energy**

©2009-2020, JGPT. All Rights Reserved 

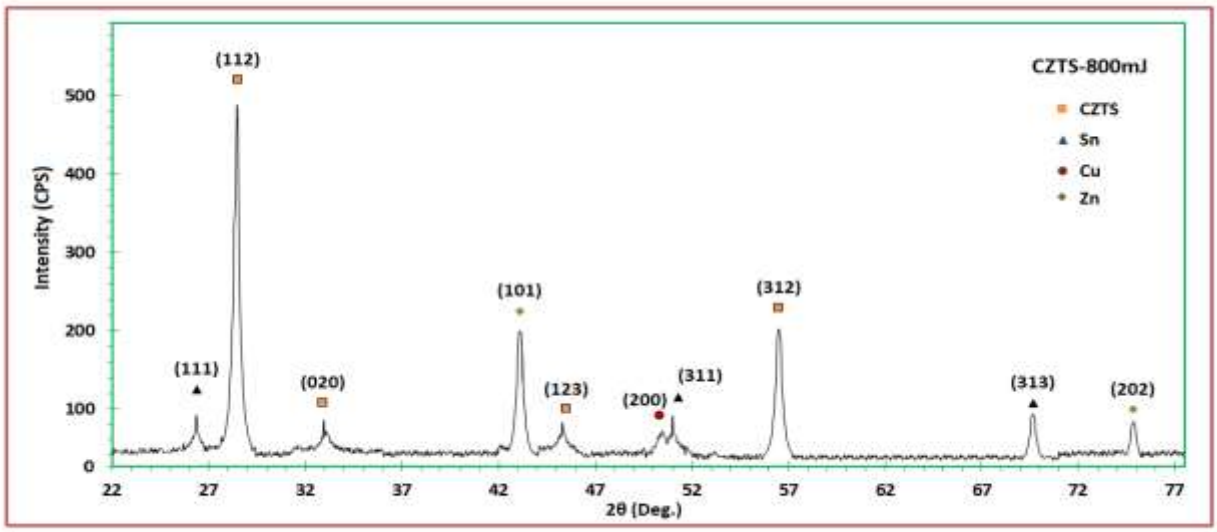


**Figure 1.5: X-ray diffraction of CZTS films prepared with 300 pulses, 1064 nm wavelength and 800 mJ laser energy**

**Table 1.1: X-ray Screening Parameters for $Cu_2ZnSnS_4$ films samples at Different Laser Energies**

| Sample | 2θ (Deg.) | FWHM (Deg.) | Int. (a.u) | d (nm) | G.S (nm) | hkl | a (nm) | c (nm) | strain (□) nm | dislocation density (□) $nm^{-2}$ |
|---|---|---|---|---|---|---|---|---|---|---|
| **CZTS 400mJ** | 28.4 | 1.36 | 561 | 3.14 | 6.03 | (112) | 8.88 | 7.24 | 0.00572 | 0.02756 |
| | 40.4 | 0.4 | 98 | 2.23 | 21.17 | (206) | 4.46 | 3.64 | 0.00163 | 0.00223 |
| | 41.96 | 1.8 | 84 | 2.15 | 4.73 | (112) | 3.72 | 3.04 | 0.00733 | 0.04479 |
| **CZTS 500mJ** | 28.49 | 1.1 | 525 | 3.13 | 7.45 | (112) | 5.42 | 4.42 | 0.00465 | 0.01802 |
| | 33.96 | 0.6 | 69 | 2.64 | 13.85 | (020) | 5.27 | 4.30 | 0.00025 | 0.00522 |
| | 46.92 | 1.6 | 134 | 1.93 | 5.41 | (312) | 6.97 | 5.69 | 0.00640 | 0.03416 |
| | 56.05 | 0.6 | 70 | 1.64 | 15.00 | (206) | 3.27 | 2.67 | 0.00231 | 0.00444 |
| | 60.5 | 2.2 | 135 | 1.53 | 4.18 | (316) | 5.51 | 4.49 | 0.00829 | 0.05728 |
| **CZTS 600mJ** | 28.4 | 1.27 | 459 | 3.14 | 6.46 | (112) | 5.43 | 4.43 | 0.00537 | 0.02403 |
| | 32.76 | 0.8 | 73 | 2.73 | 10.36 | (204) | 5.46 | 4.45 | 0.00334 | 0.00934 |
| | 45.14 | 1.4 | 99 | 2.01 | 6.15 | (123) | 5.30 | 4.33 | 0.00564 | 0.0265 |
| | 56.5 | 1.2 | 77 | 1.63 | 7.52 | (312) | 5.86 | 4.78 | 0.00461 | 0.01772 |
| | 62.7 | 0.6 | 80 | 1.48 | 15.51 | (206) | 2.96 | 2.41 | 0.00223 | 0.00416 |
| | 76.3 | 1.2 | 86 | 1.25 | 8.42 | (316) | 4.49 | 3.66 | 0.00441 | 0.01412 |
| **CZTS 700mJ** | 28.48 | 1.53 | 491 | 3.13 | 5.36 | (020) | 6.26 | 5.11 | 0.00647 | 0.03487 |
| | 32.96 | 1.6 | 165 | 2.72 | 5.18 | (220) | 9.40 | 7.67 | 0.00669 | 0.03732 |
| | 38.84 | 0.6 | 265 | 2.32 | 14.05 | (204) | 4.63 | 3.78 | 0.00246 | 0.00507 |
| | 39.97 | 0.4 | 182 | 2.25 | 21.14 | (206) | 4.50 | 3.67 | 0.00164 | 0.00224 |
| | 41.53 | 1.2 | 284 | 2.17 | 7.08 | (112) | 3.76 | 3.07 | 0.00489 | 0.01996 |
| **CZTS 800mJ** | 28.53 | 1.38 | 565 | 3.13 | 5.94 | (112) | 5.41 | 4.41 | 0.00583 | 0.02436 |
| | 32.94 | 0.4 | 72 | 2.72 | 20.72 | (020) | 5.43 | 4.43 | 0.00167 | 0.00233 |
| | 45.03 | 0.8 | 70 | 2.01 | 10.75 | (123) | 5.32 | 4.34 | 0.00322 | 0.00866 |
| | 56.5 | 0.68 | 216 | 1.63 | 13.27 | (312) | 5.86 | 4.78 | 0.00261 | 0.00569 |
| | 77.92 | 0.4 | 62 | 1.23 | 25.55 | (332) | 6.36 | 5.19 | 0.00135 | 0.00153 |

Figure (1.6a, b) shows the topography of the CZTS films in two and three dimensions prepared with a (400)mJ laser energy, Number of laser pulses 300 pulse and (1064) nm wavelength. From the topography of the film surface, a number of nanostructures were observed with a grain size of (96.00) nm, a mean square root rate (RMS) of about (7.05) nm and a surface roughness rate of (6.04) nm.

The nanoparticles are formed at this energy, which is shown by the results of RMS values.

Thus, the smallness of these values indicates the smoothness of the surface, which confirms the smallness of these graines actually because of its smallness, the surface has dense filler (Grains Packed Densely 6.04nm), the highest volume percentage is 10.39%, the aggregations rate is 27.27% and

©2009-2020, JGPT. All Rights Reserved 

the granular diameter is 80. Figure (1.6c) shows the statistical distribution of the percentages of the grain diameters in the deposition conditions above.

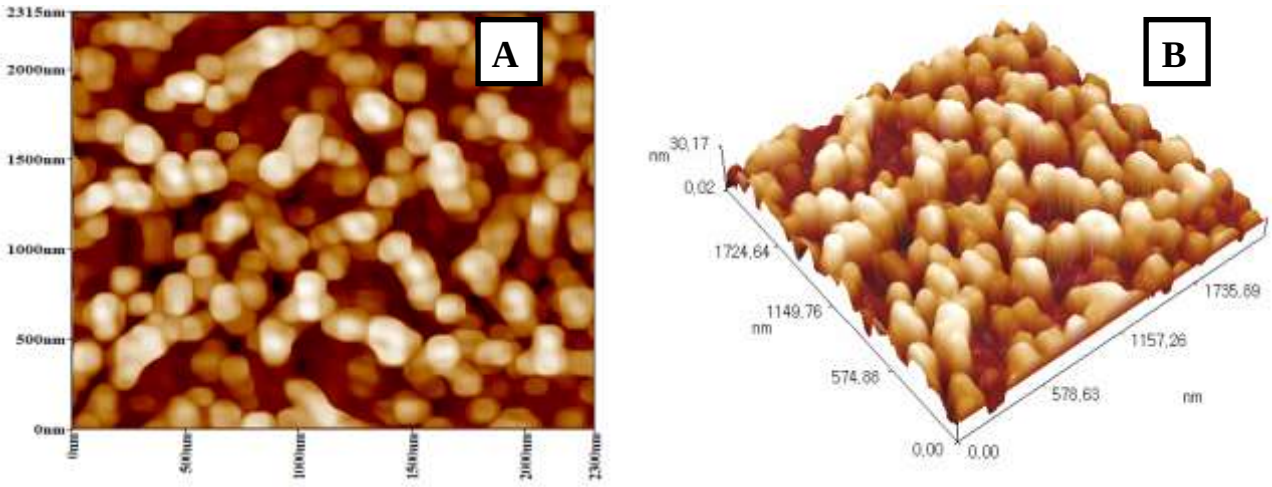


**Figure 1.6a, b: Topographic surface of CZTS films prepared with a 400 mJ laser energy, 1064 nm wavelength and number of pulses 300pulse in (a) 2-D (b) 3-D**

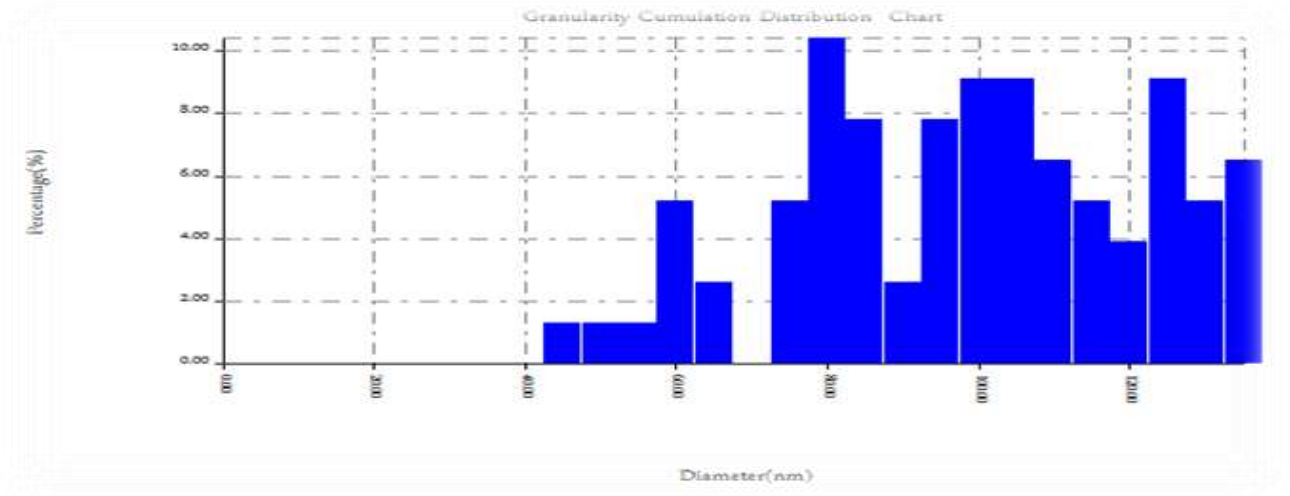


**Figure 1.6c: Statistical distribution of CZTC films for nanoparticle diameters at 400mJ laser**

Figure (1.7a, b) shows the topography of the CZTS films in two and three dimensions prepared with a (500) mJ laser energy, Number of laser pulses 300 pulse and (1064) nm wavelength. From the topography of the film surface, a number of nanostructures were observed with a grain size of (87.50) nm, a mean square root rate (RMS) of about (8.77) nm and a surface roughness rate of (7.49) nm. AFM images show a slight increase in the roughness of the measured surface through the RMS value and the highest volume percentage is 9.32%. The aggregations ratio is (46.95) and the grain diameter is (85.00) nm. Figure (1.7c) shows the statistical distribution of the percentages of the grain diameters in the deposition conditions above.

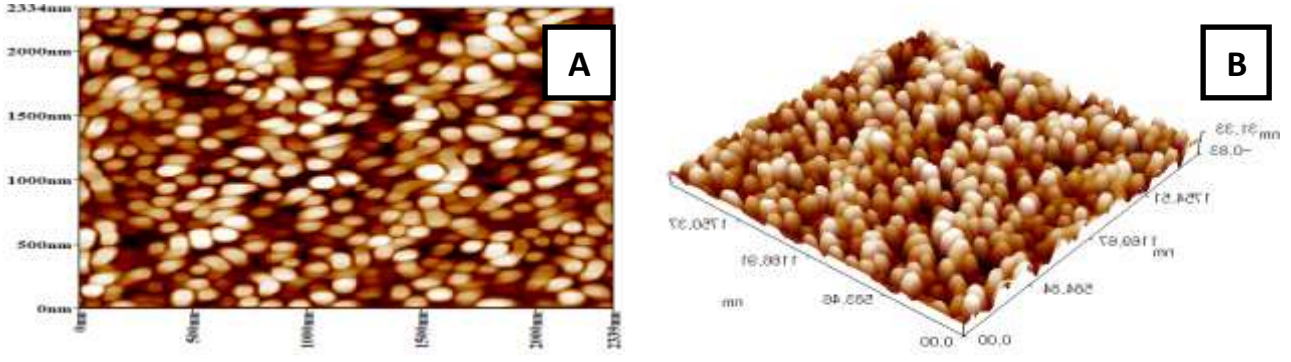


**Figure (1.7a, b) Topographic surface of CZTS films prepared with a 500 mJ laser energy, 1064 nm wavelength and number of pulses 300pulse in (a) 2-D (b) 3-D**

©2009-2020, JGPT. All Rights Reserved 

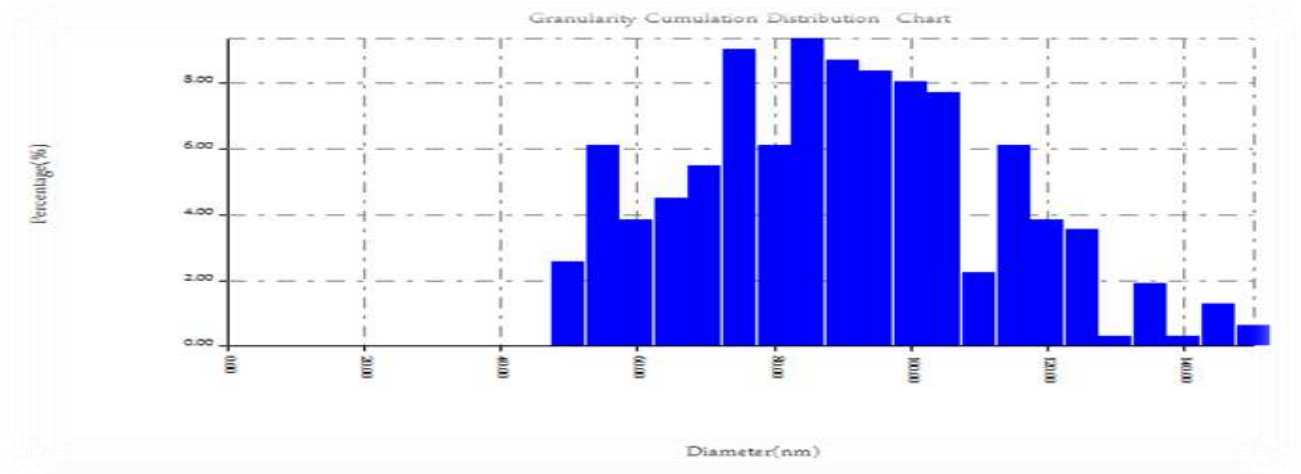


**Figure 1.7c: Statistical distribution of CZTC films for nanoparticle diameters at 500mJ laser energy**

Figure (1.8a, b) shows the topography of the CZTS films in two and three dimensions prepared with a (600) mJ laser energy, Number of laser pulses 300 pulse and (1064) nm wavelength.

From the topography of the film surface, a number of nanostructures were observed with a grain size of (59.56) nm, a mean square root rate (RMS) of about (1.88) nm and a surface roughness rate of (1.58) nm. The highest volume percentage is 25.52%, the aggregate ratio is (53.65) and the granular diameter is 60nm when the laser energy is increased (600 mJ) as in Figure (1.8a, b). AFM images showed a decrease in surface roughness than at low laser energies, indicating a decrease in grain size and the appearance of grain boundaries clearly this indicates an improved crystal structure of the film ie an improvement in films properties. Figure (4.8c) shows the statistical distribution of the percentages of the grain diameters in the deposition conditions above.

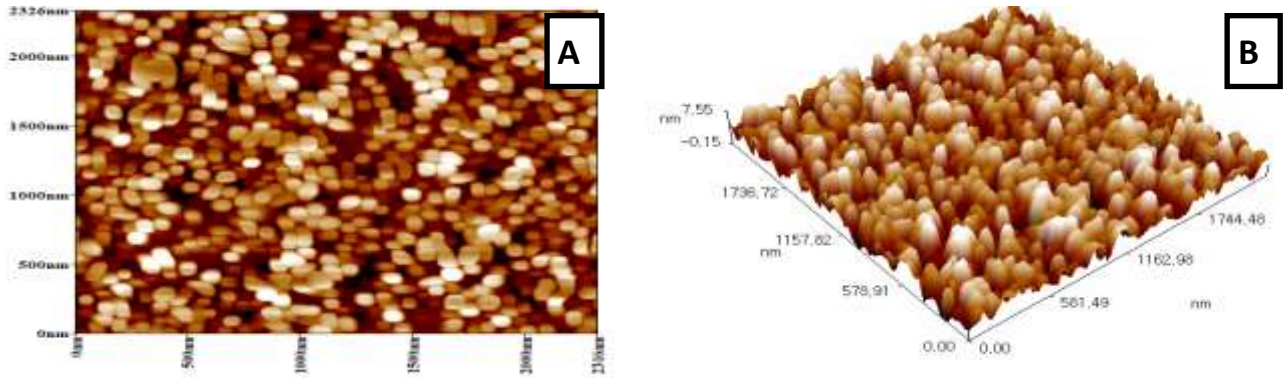


**Figure (1.8a, b) Topographic surface of CZTS films prepared with a 600 mJ laser energy, 1064 nm wavelength and number of pulses 300pulse in (a) 2-D (b) 3-D**

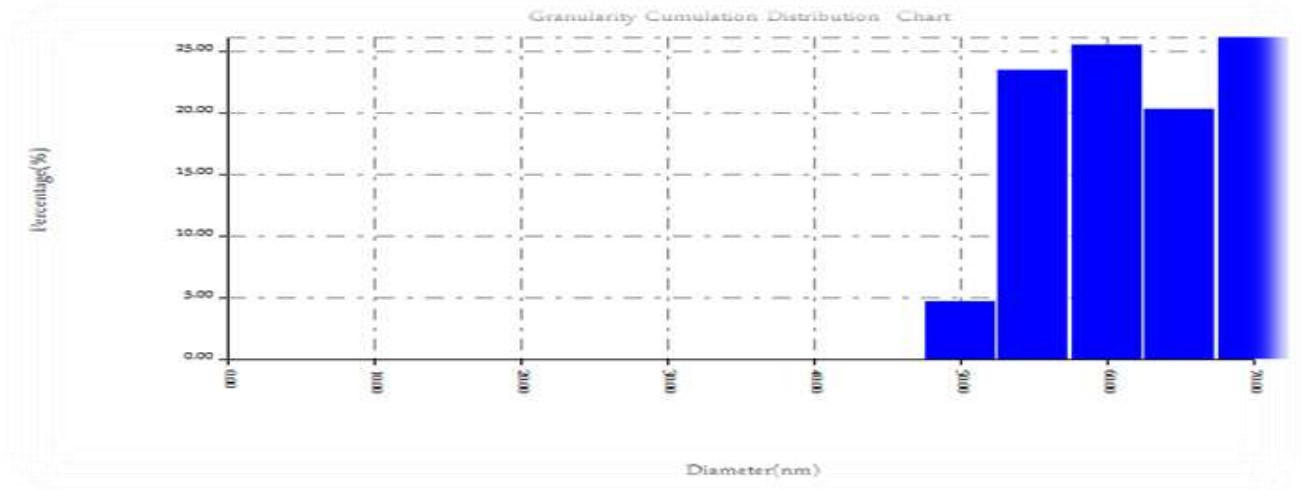


**Figure 1.8c: Statistical distribution of CZTC films for nanoparticle diameters at 600mJ laser energy**

©2009-2020, JGPT. All Rights Reserved 

Figure (4.9a, b) shows the topography of the CZTS films in two and three dimensions prepared with a (700) mJ laser energy, Number of laser pulses 300 pulse and (1064) nm wavelength. From the topography of the film surface, a number of nanostructures were observed with a grain size of (48.24) nm, a mean square root rate (RMS) of about (3.58) nm and a surface roughness rate of (3.11) nm. The highest volume percentage is 11.13%, the aggregate ratio is (56.32) and the granular diameter is 50nm. Figure (4.9c) shows the statistical distribution of the percentages of the grain diameters in the deposition conditions above.

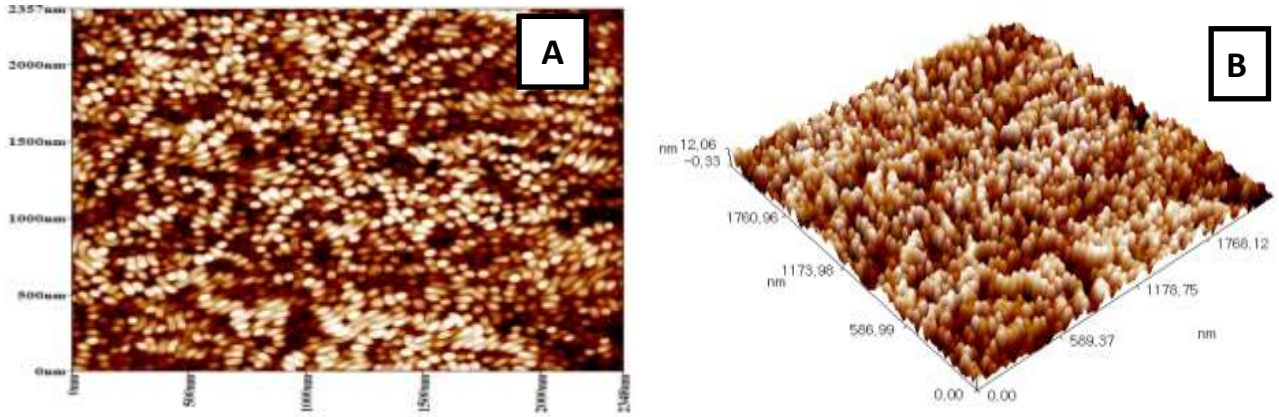


**Figure 1.9a,b: Topographic surface of CZTS films prepared with a 700 mJ laser energy, 1064 nm wavelength and number of pulses 300pulse in (a) 2-D (b) 3-D**

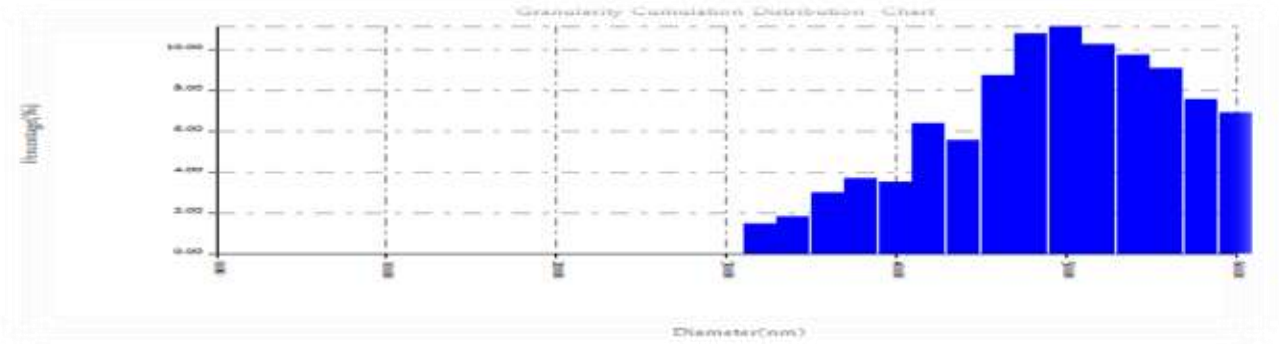

**Figure 1.9c: Statistical distribution of CZTC films for nanoparticle diameters at 600mJ laser energy**

Figure (1.10a, b) shows the topography of the CZTS films in two and three dimensions prepared with a (800) mJ laser energy, Number of laser pulses 300 pulse and (1064) nm wavelength. From the topography of the film surface, a number of nanostructures were observed with a grain size of (87.52) nm, a mean square root rate (RMS) of about (4.39) nm and a surface roughness rate of (3.66) nm. The highest volume percentage is 12.82%, the aggregate ratio is (23.93) and the granular diameter is 70nm. Figure (1.10c) shows the statistical distribution of the percentages of the grain diameters70 in the deposition conditions above.

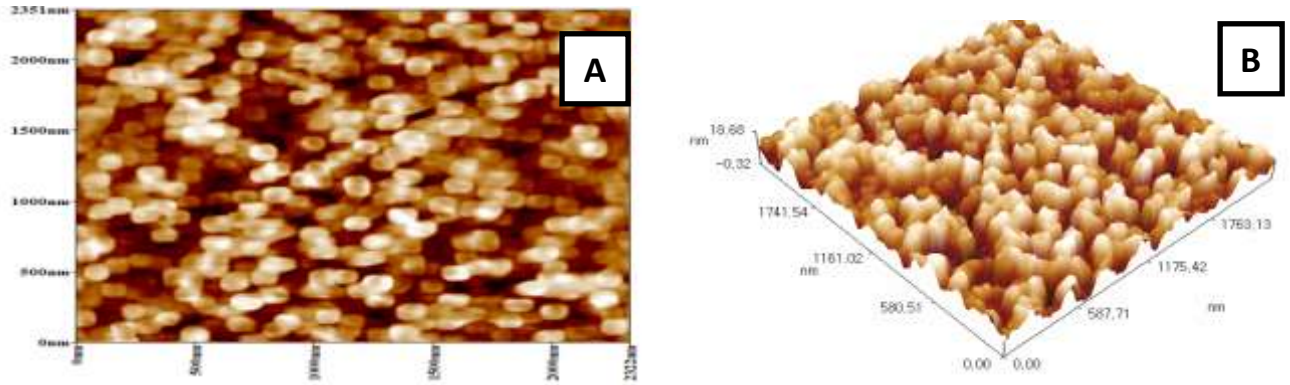


**Figure (1.10a,b) Topographic surface of CZTS films prepared with a 800 mJ laser energy, 1064 nm wavelength and number of pulses 300pulse in (a) 2-D (b) 3-D**

©2009-2020, JGPT. All Rights Reserved

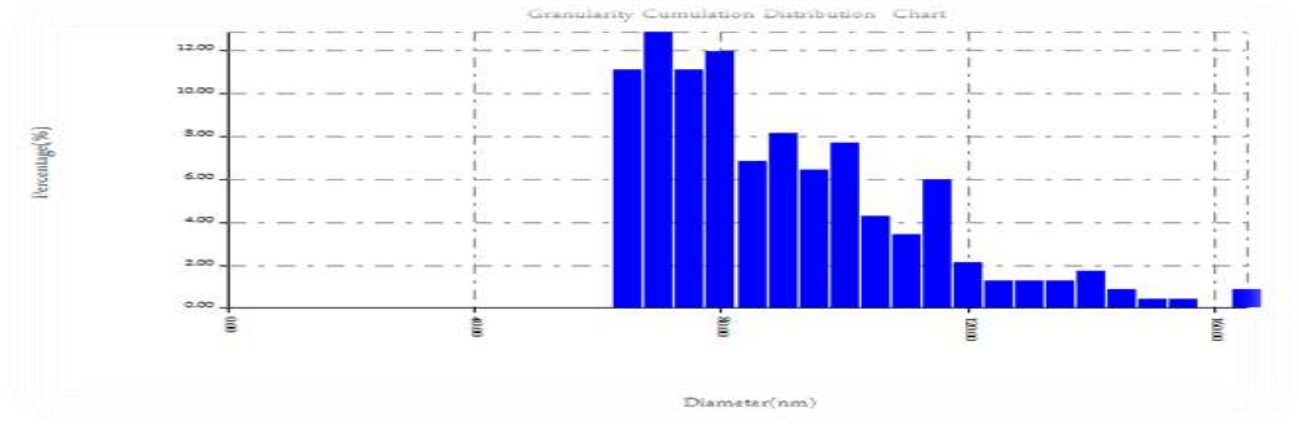


**Figure 1.10c: Statistical distribution of CZTC films for nanoparticle diameters at 600mJ laser energy**

**Table 1.2: AFM parameters for CZTS thin films at different laser energies**

| Sample | RMS (nm) | Roughness (nm) | Grain Size (nm) |
|---|---|---|---|
| $CZTS_{400mJ}$ | 7.05 | 6.04 | 96.00 |
| $CZTS_{500mJ}$ | 8.77 | 7.49 | 87.50 |
| $CZTS_{600mJ}$ | 1.88 | 1.58 | 59.56 |
| $CZTS_{700mJ}$ | 3.58 | 3.11 | 48.24 |
| $CZTS_{800mJ}$ | 4.39 | 3.66 | 87.52 |

The surface topography was studied using a scanning electron microscope of CZTS films of different laser energies (400mJ, 500mJ, 600mJ, 700mJ, 800mJ) and under pressure ($10^{-5}$) mbar, number of pulses (300) pulse and wavelength (1064) nm. Figure (1.11.a) shows the electron microscopy images of the CZTS films at laser energy (400mJ), it is noted that the grains are distributed regularly on the surface of the film with found some defects and accumulation of molecules (CZTS) in certain sites without other sites however, there are aggregations of grains and they take a spherical shape resulting from the mixing of some grains with each other due to the evaporation and deposition conditions on glass substrates. Figure (1.11.b) shows images of CZTS films at laser energy (500mJ), it is noted that there are grains take the form of spheres when the laser energy increases due to the clusters that occur on some of the grains, which increases the size of the nanoparticles others are irregular in shape, with some holes, although grouped together but not contiguous due to a number of complications due to the occurrence of the phenomenon (Coalescences), therefore, the proportion of statistical distribution of large sizes is low. Figure (1.11.c) shows images of CZTS films at laser energy (600mJ) note that when the laser energy increases in the films of the compound, some grains take small sizes and spherical shapes with the presence Some holes and change the statistical distribution of the nanoparticle diameters. Figure (1.11.d) shows images of CZTS films at laser energy (700mJ), an increase in grain size is observed and regular spherical shapes are generated as a result of increased laser energy because of the shorter bonds of the compound, it generates more film homogenization. Figure (1.11.e) shows images of the CZTS films at laser energy (800 mJ). It has been observed there is little homogeneity of film grains that take the spherical shape with an increase in grain size due to the high increase in laser energy.

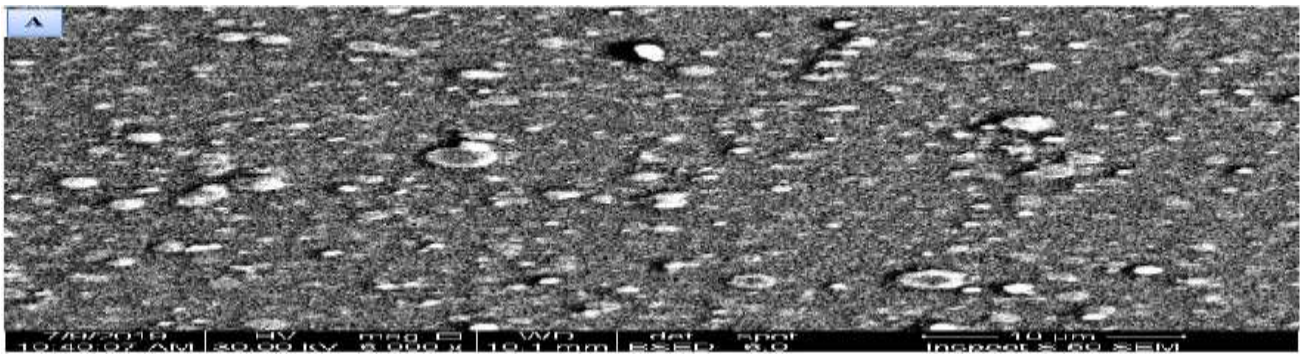

©2009-2020, JGPT. All Rights Reserved 

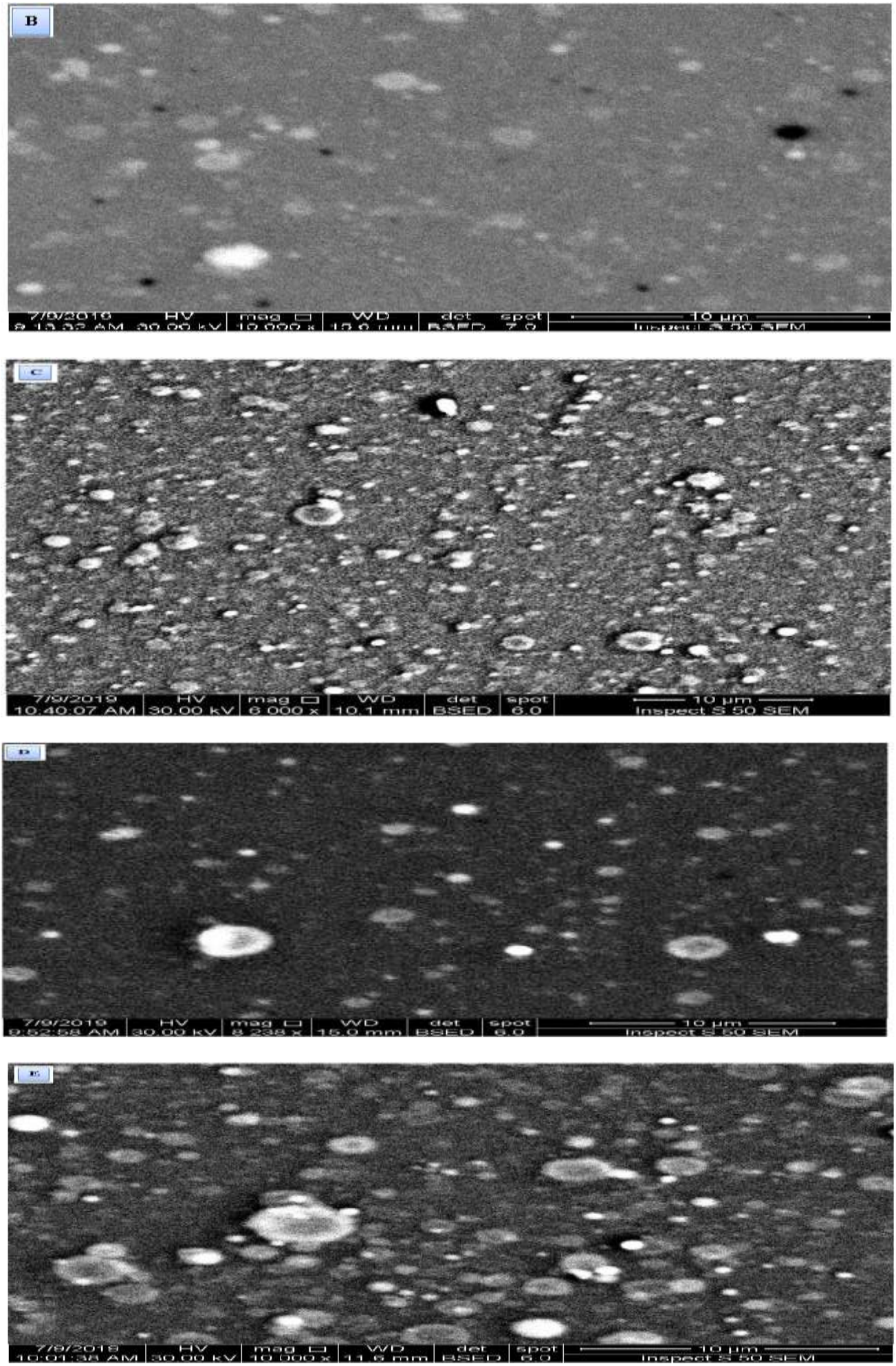


**Figure 1.11: The SEM image of the prepared films of different laser energies: (a) $CZTS_{400mJ}$, (b) $CZTS_{500mJ}$, (c) $CZTS_{600mJ}$, (d) $CZTS_{700mJ}$ and (e) $CZTS_{800mJ}$**

©2009-2020, JGPT. All Rights Reserved 

The (EDXS) spectra of the CZTS thin films of different laser energies (400mJ, 500mJ, 600mJ, 700mJ, 800mJ) are given in Figures (1.12), (1.13), (1.14), (1.15), (1.16). The EDX spectrums for all samples are clearly observable Cu, Zn, Sn and S lines. This is observed that all the films contain the elements (Cu, Zn, Sn, S) as expected, indicating formation of the $Cu_2ZnSnS_4$ films with high purity as listed in the Table (1.3).

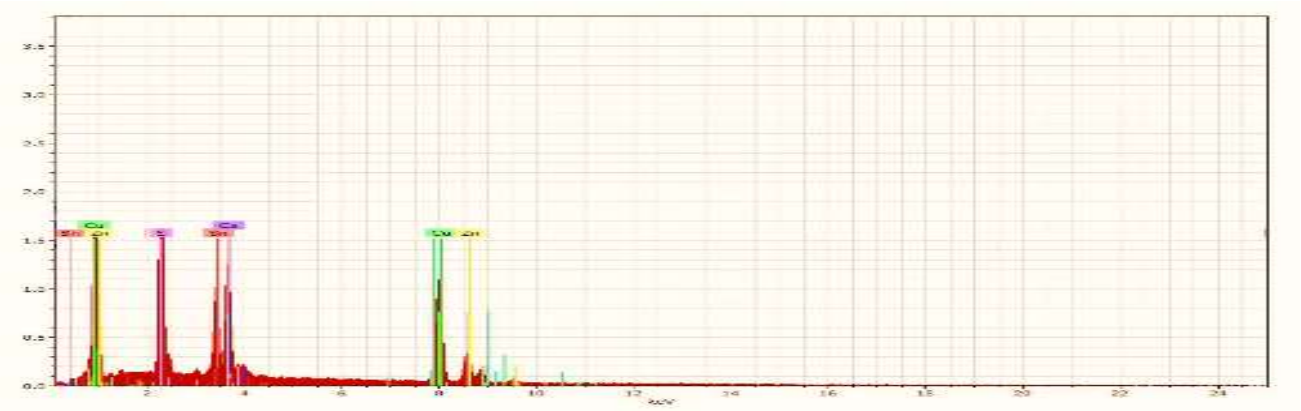

**Figure 1.12: EDX spectra of the prepared films $CZTS_{400mJ}$**

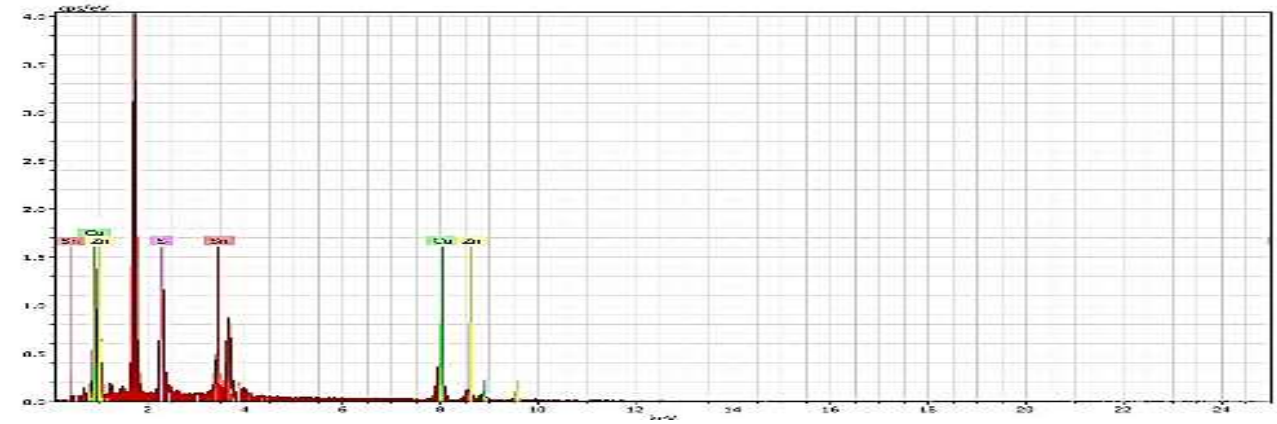

**Figure 1.13: EDX spectra of the prepared films $CZTS_{500mJ}$**

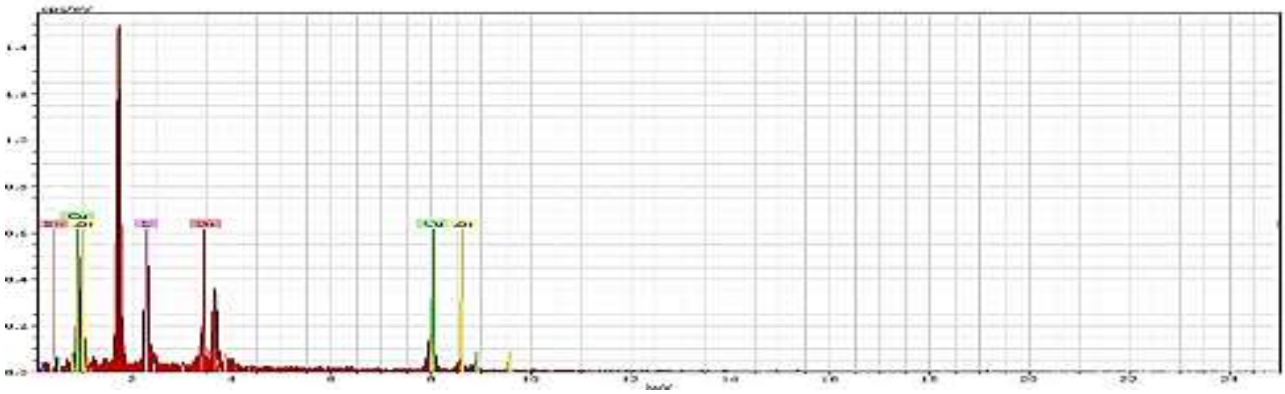

**Figure 1.14: EDX spectra of the prepared films $CZTS_{600mJ}$**

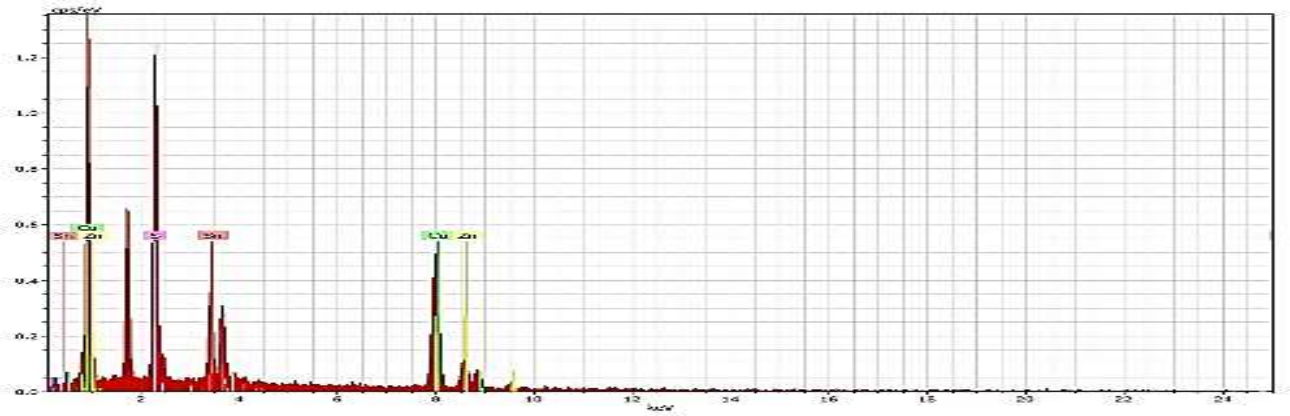

**Figure 1.15: EDX spectra of the prepared films $CZTS_{700mJ}$**

©2009-2020, JGPT. All Rights Reserved

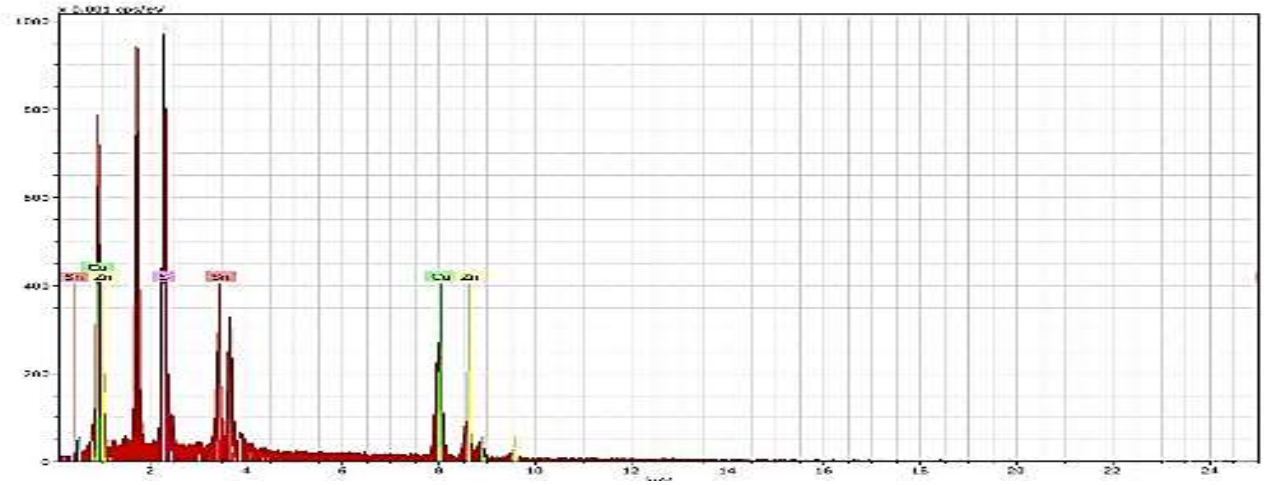

**Figure 1.16: EDX spectra of the prepared films $CZTS_{800mJ}$**

**Table 1.3: Compound percentage of the $Cu_2ZnSnS_4$ thin films**

| Sample | Compound percentage ( % ) | | | | Total |
|---|---|---|---|---|---|
| | Cu | Zn | Sn | S | |
| $CZTS_{400mJ}$ | 32.74 | 25.17 | 28.27 | 13.82 | 100 |
| $CZTS_{500mJ}$ | 22.22 | 23.49 | 40.44 | 13.85 | 100 |
| $CZTS_{600mJ}$ | 21.70 | 21.29 | 42.08 | 14.93 | 100 |
| $CZTS_{700mJ}$ | 20.88 | 16.37 | 43.06 | 19.69 | 100 |
| $CZTS_{800mJ}$ | 20.34 | 16.07 | 43.38 | 20.21 | 100 |

## Conclusions

- The method of pulsed laser deposition has proved its efficiency in preparing thin films within nanoscale ranges and at pressures ($10^{-5}$mbar).
- By x-ray diffraction study of $Cu_2ZnSnS_4$ compound films prepared by pulsed laser deposition method In different laser energies and other laser parameters constant are proven to be polycrystalline tetragonal as noted when the laser energy is increased when the process of ablation of the target CZTS The grain size increases while the strain, the dislocation density and the lattice constants ($a_o$, $c_o$) decrease.
- Through the images of the atomic force microscope (AFM) it was observed that the grain size decreases from ($CZTS_{400mJ}$-$CZTS_{700mJ}$) and then increases. There is also an increase in the surface roughness rate and the square root rate ($CZTS_{600mJ}$ - $CZTS_{800mJ}$) by increasing the laser energy when the process of ablation of the target CZTS with constant other laser parameters.
- Through scanning electron microscopy (SEM) images, the spherical shape of the nanoparticles is observed by increasing the laser energy when the process of ablation of the target CZTS with constant other laser parameters with irregular forms.
- The EDX test showed that the films contained Cu, Zn, Sn, S elements as expected, indicating the formation of high-purity CZTS films.

## References


1. Chen XG, Gong A Walsh, SH Wei (2009) "Crystal and electronic band structure of $Cu_2ZnSnX_4$ (X=S and Se) photovoltaic absorbers: First-principles insights" (PDF). Applied Physics Letters, 94 (4): 041903.
2. S Chen, XG, Gong a Walsh, S Wei (2010) "Applied physics letters," 96.
3. T Ida," Bragg's law" (2013) Chapter 1, Advanced Ceramics Research Center.
4. K Ito, T Nakazawa (1988) Electrical and optical properties of stannite-type Quaternary semiconductor thin films, Japanese Journal of Applied physics, 27: 20-94.
5. A Nagoya, R Asahi, Wahl R, G Kresse (2010) "Physical Review", 113: 202.
6. A Weber, S Schmidt, Abou D Ras, P Schobert-Bischoff, I Denks, R Mainz, HW Schock (2009) Texture inheritance in Thin film Growth of $Cu_2ZnSnS_4$, Applied Physics Letters, 95: 041-904.


©2009-2020, JGPT. All Rights Reserved 